

Original Article

Adsorption of Congo red from aqueous solution by surfactant-modified rice husk: Kinetic, isotherm and thermodynamic analysis

Chanut Bamroongwongdee*, Songsiri Suwannee, and Manit Kongsomsaksiri

*Department of Industrial Chemistry, Faculty of Applied Science,
King Mongkut's University of Technology North Bangkok, Bang Sue, Bangkok, 10800 Thailand*

Received: 9 January 2018; Revised: 28 May 2018; Accepted: 10 June 2018

Abstract

In this present work, organo-modified rice husk (SMRH) adsorbent was prepared by using cetyltrimethyl ammonium bromide (CTAB) for removing Congo red (CR), a model anionic dye, from aqueous solution. The FTIR analysis indicated that CTAB was adsorbed onto the surface of rice husk. The adsorption was found to be favored at a lower pH. The amount of CR uptake was found to increase with increasing the initial CR concentration and contact time but decrease with increasing the amount of adsorbent. The equilibrium adsorption data were fitted well with the Langmuir model. The adsorption kinetics showed that CR adsorption onto SMRH followed the pseudo-second-order model. It was found that intra-particle diffusion was not the only rate-determining step. Thermodynamic studies revealed that CR adsorption onto SMRH was spontaneous and endothermic in nature.

Keywords: adsorption, Congo red, modified rice husk, kinetics, thermodynamics

1. Introduction

One major pollution problem stems from the release of large volumes of wastewater from various industries, such as textile, paper, printing, cosmetics and pharmaceuticals, due to the presence of a large number of synthetic dyestuffs (Roy & Mondal, 2017; Xi *et al.*, 2013). These colored compounds have several negative effects, not only on the aquatic life due to reduction of light penetration and photosynthetic activity, but also on human beings because of their toxicity and carcinogenic nature (Munagapati & Kim, 2016).

Congo red (CR) is a benzidine-based anionic diazo dye, commonly used in the textile, paper, printing and other industries (Mane & Babu, 2013). This synthetic dye is highly water-soluble and not easily biodegraded or photodegraded due to its structural stability (Zenasni, Meroufel, Merlin, & George, 2014). It is also known to metabolize to carcinogenic products and causes irritation to the skin, eyes and gastrointestinal tract (Roy & Mondal, 2017). Therefore, dye removal

from wastewater is an important issue. Several physico-chemical and biological methods such as coagulation-flocculation, ozonation, advanced oxidation, liquid-liquid extraction, biosorption and adsorption have been widely employed for the decolorization of dye containing wastewater (Zenasni, Meroufel, Merlin, & George, 2014). Among these techniques, adsorption is a well-known separation technique that provides an effective and attractive treatment method for the removal of soluble organic pollutants like dyes from wastewater. This approach offers several advantages including simple design, easy operation and handling, insensitivity to toxic substances, and low operating costs (Mane & Babu, 2013). Activated carbon is a highly efficient adsorbent for the removal of various dissolved organic pollutants from wastewater; however, the high cost of commercial activated carbon limits its use in wastewater treatment. Therefore, there is a need to search for low-cost and effective adsorbents. Recently, agricultural by-products and wastes, such as Eucalyptus wood saw dust (Mane & Babu, 2013), peanut husk (Sadaf & Bhatti, 2014), wheat straw (Zhang *et al.*, 2014), and magnolia leaf (Yu *et al.*, 2016), have been used as alternative adsorbents to remove various dyes from aqueous solutions.

Rice husk is an abundant low-cost agricultural by-product from the rice milling industry. Chemical composition

*Corresponding author

Email address: chanut.b@sci.kmutnb.ac.th

of rice husk is similar to organic fibers, consisting of cellulose, lignin, hemicellulose, and silicon dioxide (Ludueña, Fasce, Alvarez, & Stefani, 2011), and it has been used as an adsorbent to remove several dyes from aqueous solution (Safa, & Bhatti, 2011). However, it is well-known that natural agricultural by-products have low adsorption capacity, which can be enhanced through physical and chemical modifications (Munagapati & Kim, 2016). Some researchers used a cationic surfactant to modify an agricultural by-product to remove anionic ions. Cetyltrimethyl ammonium bromide (CTAB) was used to modify some agricultural by-products such as silkworm exuviae (Chen, Zhao, Wu, & Dai, 2011), sawdust (Ansari, Seyghali, Mohammad-khah, & Zanjanchi, 2012) and wheat straw (Zhang *et al.*, 2014), with promising results in removal of anionic dyes. However, few studies have assessed using rice husk modified by CTAB for dye adsorption. Thus, this study was conducted to evaluate CTAB modified rice husk for the removal of CR from an aqueous solution. The effects of various parameters on the adsorption, such as solution pH, contact time and initial dye concentration, were investigated. The adsorption isotherm, kinetics, and a thermodynamic study have been carried out to determine the mechanism of CR adsorption onto modified rice husk.

2. Materials and Methods

2.1 Materials

Congo red (M.W. = 696.68 g/mol) was provided by Ajax Finechem Pty Ltd. and used without further purification. The stock dye solution of 1.0 g/L was prepared by dissolving the required amount of CR in distilled water. The other solutions of desired concentration were prepared by diluting from the stock solution. Cetyltrimethyl ammonium bromide (M.W. = 364.46 g/mol) was purchased from Ajax Finechem Pty Ltd. All the reagents used in this study were of analytical grade and all of the solutions were prepared with distilled water.

2.2 Biosorbent preparation

Rice husk (RH) collected from a local rice mill was washed repeatedly with tap water for several times to remove the adhering dirt. Then it was washed with distilled water several times and dried in an oven at 110°C for 3 h. Dry rice husk was ground and then sieved to obtain particle size in the range 90-354 µm (175 to 45 mesh).

To modify the rice husks, 15 g of the dried rice husk was mixed in 200 mL of CTAB solution (1.5 wt%). The suspension was then shaken in shaker machine at 120 rpm at room temperature for 24 h. The mixture was filtered and washed several times with distilled water until no bromide ions were detected by adding a 0.1M AgNO₃ solution to the filtrate. The sample was dried in an oven at 110°C for 12 h and stored in an air-tight container. The obtained product was labelled as surfactant-modified rice husk (SMRH).

2.3 Characterization of SMRH

FTIR spectra of RH and SMRH were recorded with a Fourier transform infrared absorption spectrophotometer

(FTIR-2000, Perkin Elmer) using the KBr disc method. The sample spectra were collected over the range 4000-400 cm⁻¹ with a resolution of 4 cm⁻¹.

The pH-zero point of charge (pH_{PZC}) was measured by preparing 0.01 M NaCl solution at pH 3-11. 0.2 g of the adsorbent was added to 50 mL of each solution. After a contact time of 24 h, the final pH was measured. The difference between the initial and final pH was plotted against the initial pH. The pH_{PZC} is the point where pH_{final} - pH_{initial} = 0 (Kaur, Rani, & Mahajan, 2013).

2.4 Batch adsorption experiments

The experiments on CR adsorption by SMRH were of batch type at 303, 313, 323, and 333 K. The adsorption experiments were conducted with the four initial concentrations 25, 50, 75, and 100 mg/L of CR. 0.5 g of SMRH was added to 50 mL of a CR solution of known concentration in a 250 mL Erlenmeyer flask. The suspension was then shaken in a water-bath shaker at 120 rpm. The dye solutions were separated from the adsorbent using centrifugation, for samples collected at predetermined time intervals. The supernatant concentration was determined using a UV-vis spectrophotometer at the maximum absorbance wavelength of 520 nm. The effect of pH on the dye adsorption was studied by adjusting pH from 3 to 11 using 0.1M HCl or 0.1M NaOH solution.

The amount of CR adsorbed at time *t* and the percentage removal of CR by SMRH were calculated using the following equations:

$$q_t = \frac{(C_0 - C_t) V}{W} \quad (1)$$

$$\% \text{ CR Removal} = \frac{C_0 - C_t}{C_0} \times 100 \quad (2)$$

where *C*₀ and *C*_{*t*} (mg/L) are the CR concentrations at initial and a given time *t*, respectively. *V* (L) is the volume of dye solution, and *W* (g) is weight of the adsorbent.

2.5 Adsorption kinetics studies

Adsorption kinetics informs about the adsorption mechanisms and rate-determining steps. In order to investigate the mechanism of the dye adsorption from aqueous solution, various kinetic models were fitted to experimental data.

In the present work, the pseudo-first-order, pseudo-second-order, Elovich, Bangham's, and intra-particle diffusion kinetic models were tested for their applicability to CR adsorption onto SMRH. The suitability of the kinetic models was evaluated based on the linear regression coefficient of determination (*R*²).

2.5.1. Pseudo-first-order kinetic model

The linearized form of the pseudo-first-order model is (Roy, & Mondal, 2017):

$$\ln(q_e - q_t) = \ln q_e - k_1 t \quad (3)$$

where q_e (mg/g) is the amount of CR adsorbed at equilibrium, q_t (mg/g) is the amount of CR adsorbed at any time t (min) and k_1 (1/min) is the pseudo-first-order rate constant.

A plot of $\ln(q_e - q_t)$ versus t yields a straight line whose slope and y-intercept can be used to determine the pseudo-first-order rate constant (k_1) and the equilibrium adsorption density (q_e) respectively.

2.5.2. Pseudo-second-order kinetic model

The linearized form of the pseudo-second-order model is (Lin *et al.*, 2013):

$$\frac{t}{q_t} = \frac{1}{k_2 q_e^2} + \frac{1}{q_e} t \quad (4)$$

where k_2 (g/mg·min) is the pseudo-second-order rate constant.

A plot of t/q_t against t gives a straight line from which q_e and k_2 can be determined from the slope and y-intercept.

2.5.3. Elovich equation

The simple Elovich model equation is generally expressed as follows (Tamilselvi, Asaithambi, & Sivakumar, 2016):

$$q_t = \frac{1}{b} \ln(ab) + \frac{1}{b} \ln t \quad (5)$$

where a (mg/g·min) is the initial adsorption rate of the Elovich equation and b (g/mg) is another constant related to the extent of surface coverage and activation energy for chemisorption.

The slope and y-intercept of the linear plot of q_t versus $\ln t$ were used to determine the values of the constants a and b .

2.5.4. Intra-particle diffusion model

The intra-particle diffusion model has been applied to elucidate the diffusion mechanism, and it is expressed as (Weber Jr., & Morris, 1963):

$$q_t = k_{id} t^{1/2} + C \quad (6)$$

where k_{id} (mg/g·min^{1/2}) is the intra-particle diffusion rate constant and constant C (mg/g) relates to the width of the boundary layer. According to this model, the plot of q_t versus $t^{1/2}$ should be linear and pass through the origin, if the intra-particle diffusion is the only rate-controlling step (Tamilselvi, Asaithambi, & Sivakumar, 2016).

2.6 Thermodynamic studies

To further assess the adsorption process taking place between CR and SMRH, thermodynamic parameters such as standard Gibbs free energy change (ΔG^0), standard enthalpy change (ΔH^0), and standard entropy change (ΔS^0) were

determined. These parameters were determined using the following equations (Baek, Ijagbemi, O, & Kim, 2010; Tamilselvi, Asaithambi, & Sivakumar, 2016):

$$\Delta G^0 = -RT \ln K_0 \quad (7)$$

$$K_0 = \frac{C_a}{C_e} = \frac{C_0 - C_e}{C_e} = \frac{C_0}{C_e} - 1 \quad (8)$$

$$\Delta G^0 = \Delta H^0 - T\Delta S^0 \quad (9)$$

$$\ln K_0 = -\frac{\Delta G^0}{RT} = -\frac{\Delta H^0}{R} \frac{1}{T} + \frac{\Delta S^0}{R} \quad (10)$$

where R (8.314 J/mol.K) is the universal gas constant, T (K) is the absolute temperature, K is the equilibrium constant, and C_e (mg/L) is the equilibrium CR concentration. The values of ΔH^0 and ΔS^0 were determined from the slope and intercept of the van't Hoff plot (i.e., plot of $\ln K_0$ versus $1/T$), respectively.

3. Results and Discussion

3.1 Characterization

The FTIR spectra of RH and SMRH are presented in Figure 1. The spectrum of the adsorbent displays many adsorption peaks, reflecting the complex nature of the materials. The broad and strong band located at 3424 cm⁻¹ was attributed to -OH stretching vibrations, indicating the presence of -OH groups in the cellulose, hemicellulose and lignin (Sadaf, & Bhatti, 2014). The peak at 2920 cm⁻¹ was attributed to stretching vibrations of C-H bond in a methylene (-CH₂) group (Pathania, Sharma, & Siddiqi, 2016). The peaks located at 1734 and 1647 cm⁻¹ were assigned to C=O bonds in

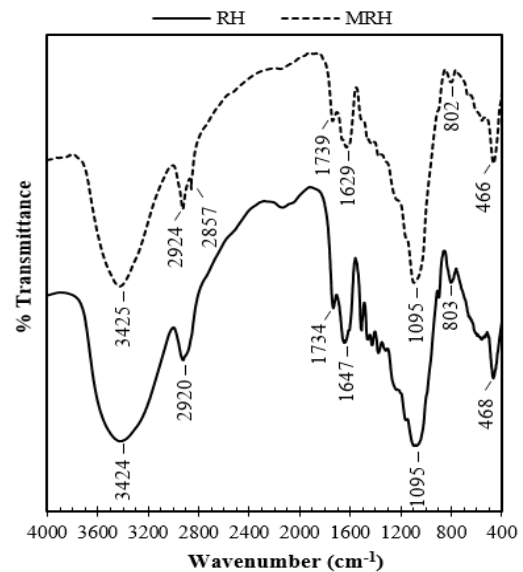


Figure 1. FTIR spectra of (a) RH and (b) SMRH.

carboxylic groups (Munagapati & Kim, 2016). The peak at 1095 cm^{-1} could be assigned to stretching vibrations of C–OH bond in cellulose. The higher intensity at 1095 cm^{-1} was probably due to the superposition of C–OH stretching vibrations in the $1000\text{--}1200\text{ cm}^{-1}$ range with Si–O stretching vibrations. The peak at 803 cm^{-1} was due to stretching vibrations of Si–O bond and the peak at 468 cm^{-1} belonged to bending vibrations of siloxane bonds (Si–O) (Tavlieva, Genieva, Georgieva, & Vlaev, 2013).

Comparison of FTIR spectra for RH and SMRH shows that the adsorption band of –CH_3 at 2923 cm^{-1} was stronger while the shoulder peak of –CH_2 at 2857 cm^{-1} was slightly reduced. This was due to increased aliphatic carbon content (from CTAB) in the SMRH, indicating CTAB on SMRH surfaces.

3.2 Batch biosorption studies

3.2.1. Effect of initial solution pH

Figure 2 shows that the maximum CR sorption was at pH 3.0 followed by significant decrease in CR sorption with increasing pH. The maximum sorption capacity of CR was found to be 7.57 mg/g at the optimum pH. The CR removal by SMRH decreased from 78.64 to 56.26% over pH range 3.0–11.0. At low pH, the SMRH surfaces are positively charged, increasing CR removal by electrostatic attraction between the positively charged surface of SMRH and anionic CR. On the other hand, lower CR adsorption at higher pH may be due to the presence of hydroxide ions competing with the sulfonate groups (–SO_3^-) of CR for biosorption sites. A similar result has been observed for CR adsorption in prior literature (Xi *et al.*, 2013). In order to not create complications with pH adjustments, CR solutions without pH adjustment were used. The CR solution had pH of 6.6–6.8.

The trends in these experiments could be further confirmed on the basis of pH_{PZC} , indicating the type of surface active centers and the adsorption ability of the surface. The pH_{PZC} of SMRH was 5.0, as shown in Figure 3. This indicates that at $\text{pH} < 5.0$, SMRH surfaces are positively charged, which improves anionic dye removal by electrostatic attraction, whereas at $\text{pH} > 5.0$ the SMRH surfaces become negatively charged and electrostatically repel the CR anions. So, anionic dye adsorption is favored at $\text{pH} < \text{pH}_{\text{PZC}}$, where the SMRH surface becomes positively charged.

3.2.2. Effect of adsorbent dosage

The removal of CR increased from 24.04% to 75.29% on increasing the SMRH dose from 2 to 20 g/L (Figure 4). Likely a higher SMRH dose provided more adsorption sites to which the dye molecules can attach (Dawood & Sen, 2012). However, the adsorption uptake of CR decreased from 12.08 mg/g to 3.81 mg/g with increasing adsorbent dose. This is probably due to a split in the concentration gradient between adsorbate and adsorbent. Therefore, the amount of dye adsorbed onto unit weight of adsorbent decreased with increasing the adsorbent mass, decreasing q_e with adsorbent mass concentration (Dawood & Sen, 2012; Roy & Mondal, 2017).

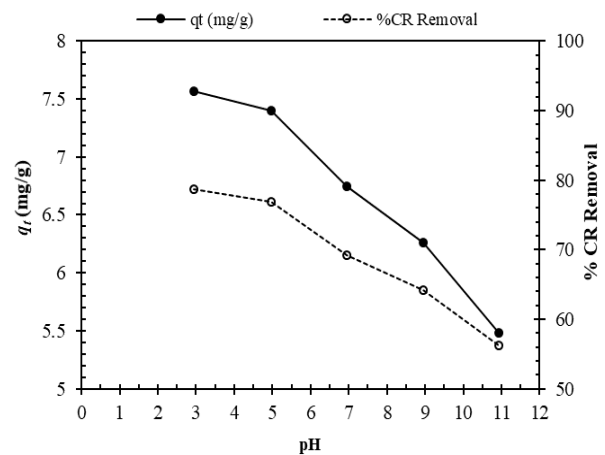


Figure 2. Effect of initial pH on CR adsorption by SMRH (C_0 : 100 mg/L, adsorption dosage: 10 g/L, pH: 3–11, Temp: 303 K, contact time: 210 min).

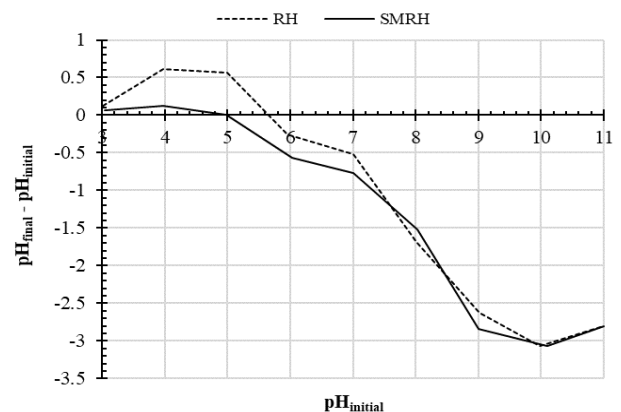


Figure 3. Point of zero charge of RH and SMRH.

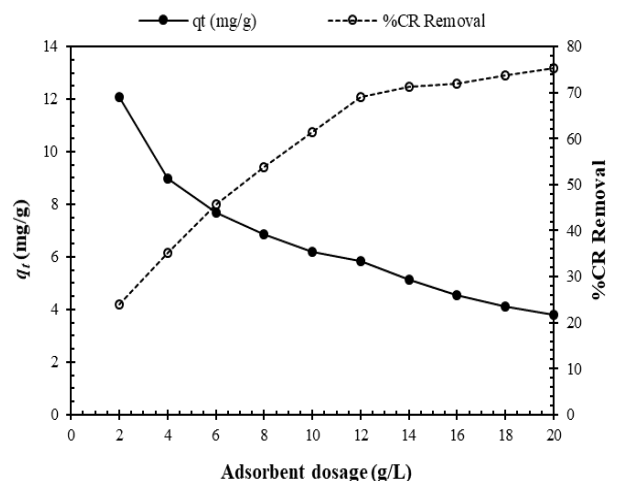


Figure 4. Effect of adsorbent dosage on CR adsorption by SMRH (C_0 : 100 mg/L, adsorption dosage: 2–20 g/L, pH: 6.6–6.8, Temp: 303 K, contact time: 210 min).

3.2.3. Effect of initial dye concentration

As shown in Figure 5, the CR removal decreased with initial CR concentration in the biosorption process. This is consistent with previous studies reported in the literature (Pathania, Sharma, & Siddiqi, 2016; Xi *et al.*, 2013), and can be attributed to the limited number of vacant adsorption sites on SMRH, which become saturated at a certain dye concentration (Xi *et al.*, 2013). Moreover, the adsorption capacity increased rapidly with initial dye concentration, which may be due to an increase in the concentration gradient (Mane & Babu, 2013).

3.2.4. Effect of contact time

Figure 6 shows that the adsorption capacity increased with contact time at all initial dye concentrations, and the equilibrium was attained within 120 min. The equilibrium time increased from 30 to 120 min on increasing the initial dye concentration from 25 to 100 mg/L. This is probably due to competition for the surface active sites at higher adsorbate concentration slowing down the equilibration (Nandi *et al.*, 2008). In addition, the adsorbed amount rapidly increased in the beginning and gradually approached equilibrium. The rapid initial adsorption is probably due to the availability of the active sites on the adsorbent surface. After a period, the remaining active sites cannot be occupied because of repulsive forces between the dye molecules on the adsorbent surface and in the bulk phase (Roy & Mondal, 2017). Another reason is that the biosorbent surface for dye adsorption was large in the initial stage and then dye molecules on the surface slowly diffused into the interior sites of the adsorbent particles (Pathania, Sharma, & Siddiqi, 2016).

3.3 Adsorption kinetics

Adsorption kinetics models are important for understanding the kinetic behaviour and assessing the rate-limiting step. The pseudo-first-order, pseudo-second-order, Elovich, and intra-particle diffusion models were applied to CR adsorption onto SMRH.

The values of k_1 , R^2 , $q_{e,exp}$ and $q_{e,cal}$ for the pseudo-first-order model at different CR concentrations were evaluated from Figure 7a and are presented in Table 1. This table shows that the experimental data did not agree with the pseudo-first-order model, as the R^2 ranged from 0.2005 to 0.9482. Moreover, the theoretical $q_{e,cal}$ values for the pseudo-first-order model are significantly lower than the experimental $q_{e,exp}$ values.

The experimental kinetic data were then analysed using the pseudo-second-order model, as shown in Figure 7b. The R^2 for the pseudo-second-order model was significantly better than for the pseudo-first-order model, and the theoretical $q_{e,cal}$ and experimental $q_{e,exp}$ values are very close to each other. Hence, CR adsorption onto SMRH can be well described by the pseudo-second-order model (Pathania, Sharma, & Siddiqi, 2016). The k_2 decreased from 1.0990 to 0.0106 min^{-1} on increasing the initial CR concentration. This phenomenon may be due to lesser competition for the adsorption sites at lower initial CR concentration. At higher initial CR concentration, the competition for the adsorption

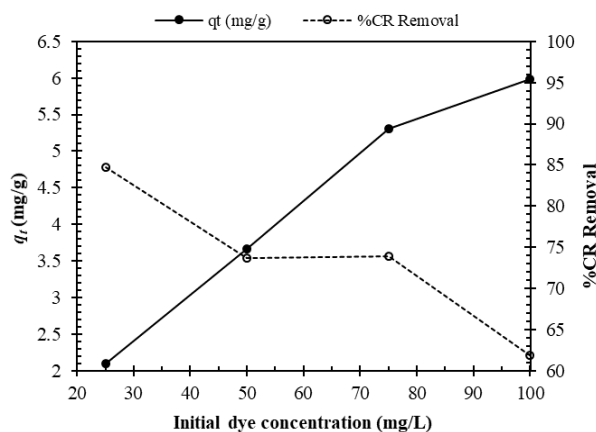


Figure 5. Effect of initial concentration on CR adsorption by SMRH (C_0 : 25–100 mg/L, adsorption dosage: 10 g/L, pH: 6.6–6.8, Temp: 303 K, contact time: 210 min).

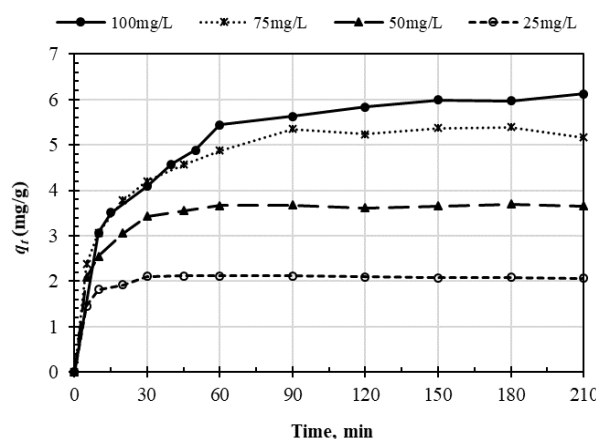


Figure 6. Effect of contact time on CR adsorption by SMRH (C_0 : 25–100 mg/L, adsorption dosage: 10 g/L, pH: 6.6–6.8, Temp: 303 K, contact time: 0–210 min).

sites will be stronger, and the adsorption rates were consequently decreased (Dawood & Sen, 2012).

The Elovich equation is used to describe chemisorption. The initial adsorption rate (a) decreased from 7832.0595 to 2.0796 $\text{mg/g}\cdot\text{min}$ on increasing the initial CR concentration. This is consistent with the results obtained from the pseudo-second-order model. The R^2 was between 0.6458 and 0.9689, indicating that CR adsorption onto SMRH did not follow the Elovich equation.

The transfer rate of dyes from aqueous solution to biosorption surfaces may be controlled by film diffusion, intra-particle diffusion, or by a combination of both mechanisms. If the diffusion (internal surface and pore diffusion) of dye molecules inside the adsorbent is the rate-controlling step, then the Weber-Morris plot of q_t versus $t^{1/2}$ should show a linear relationship in the experimental data. Figure 7d shows that these curves are not linear over the whole time range. This indicates that CR adsorption onto SMRH was controlled by more than one type of diffusion process. This plot can be separated into two linear regions. In the first linear region, the dye molecules diffused from bulk solution to external surface of SMRH and mass transfer rate was very fast. This could be

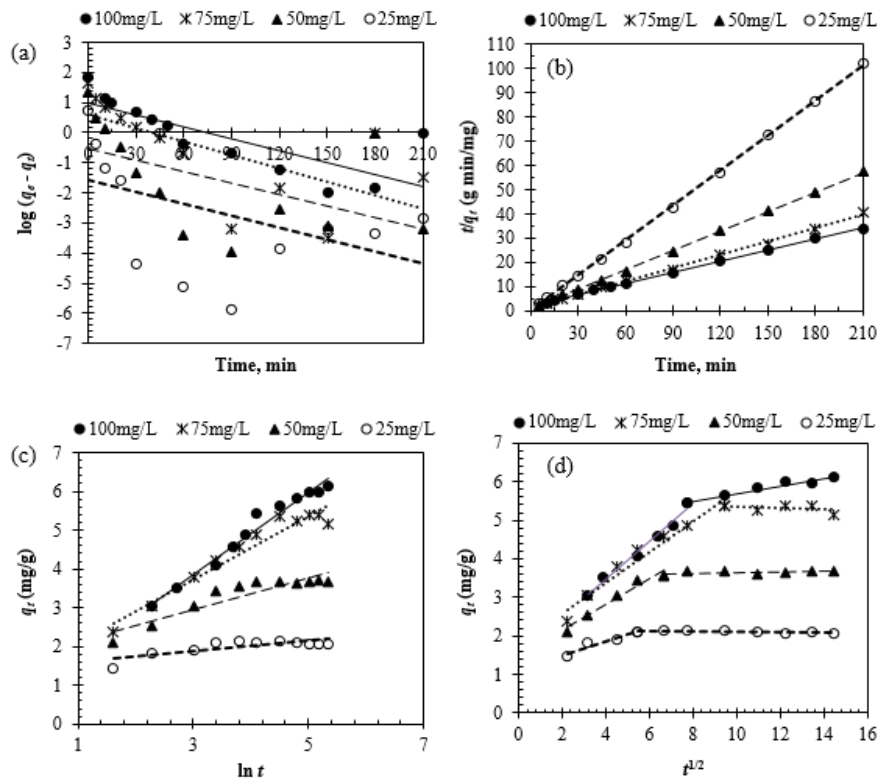


Figure 7. (a) Pseudo-first-order kinetics, (b) Pseudo-second-order kinetics, (c) Elovich kinetic model, and (d) Intra-particle diffusion kinetic model for CR removal by SMRH (C_0 : 25–100 mg/L, adsorption dosage: 10 g/L, pH: 6.6-6.8, Temp: 303 K, contact time: 0–210 min).

Table 1. Kinetic parameters for the removal of CR by SMRH (C_0 : 25–100 mg/L, adsorption dosage: 10 g/L, pH: 6.6-6.8, Temp: 303 K, contact time: 0–210 min).

Pseudo-first-order				
C_0 (mg/L)	$q_{e,exp}$ (mg/g)	$q_{e,calc}$ (mg/g)	k_1 (min^{-1})	R^2
25	2.116	0.1552	0.0120	0.2005
50	3.694	0.7372	0.0198	0.5727
75	5.394	2.0975	0.0199	0.6153
100	6.127	3.6577	0.0203	0.9482
Pseudo-second-order				
C_0 (mg/L)	$q_{e,calc}$ (mg/g)	k_2 ($\text{g/mg}\cdot\text{min}^{-1}$)	R^2	
25	2.0826	1.0990	0.9997	
50	3.7362	0.0837	0.9997	
75	5.5179	0.0241	0.9980	
100	6.5175	0.0106	0.9990	
Elovich				
C_0 (mg/L)	a ($\text{mg/g}\cdot\text{min}$)	b (g/mg)	R^2	
25	7832.0595	7.4681	0.6458	
50	30.5698	2.4746	0.8388	
75	3.9631	1.2244	0.9450	
100	2.0796	0.9519	0.9689	
Intra-particle diffusion				
C_0 (mg/L)	$k_{id,1}$ ($\text{mg/g}\cdot\text{min}^{1/2}$)	C_1 (mg/g)	R^2	
25	0.1833	1.1176	0.9041	
50	0.3361	1.4526	0.9561	
75	0.3991	1.7871	0.9619	
100	0.4875	1.5255	0.9874	
Intra-particle diffusion				
C_0 (mg/L)	$k_{id,2}$ ($\text{mg/g}\cdot\text{min}^{1/2}$)	C_2 (mg/g)	R^2	
25	-0.0055	2.149	0.7372	
50	0.0087	3.5498	0.2985	
75	0.0165	5.5018	0.1102	
100	0.0997	4.6954	0.9639	

attributed to boundary layer diffusion. The second stage of adsorption was very slow, where the intra-particle diffusion of CR into pores is the rate-limiting step (Mane & Babu, 2013). Moreover, the plots do not give straight lines passing through the origin (i.e., $C \neq 0$), indicating that intra-particle diffusion was involved in the adsorption process but was not the only rate-limiting step (Dawood & Sen, 2012). In Table 1, both k_{id} and C_i increase with initial CR concentration. An increase in the initial CR concentration will produce a higher concentration gradient resulting in faster diffusion and quicker adsorption (Nassar, Daifullah, Kelany, & Farah, 2015).

3.4 Adsorption isotherms

The adsorption isotherm is important for the description of the equilibrium nature of adsorption. It describes how the adsorbate molecules interact with the adsorbent and gives an idea of the adsorption capacity of the adsorbent (Dawood & Sen, 2012). In this work, two well-known models, the Langmuir and Freundlich isotherms, were chosen to investigate the adsorption behavior.

$$\text{Langmuir, } \frac{C_e}{q_e} = \frac{1}{q_m K_L} + \frac{1}{q_m} C_e \quad (12)$$

$$\text{Freundlich, } \log q_e = \log K_F + \frac{1}{n} \log C_e \quad (13)$$

where q_m (mg/g) is the maximum monolayer adsorption capacity and K_L (L/mg) is the Langmuir isotherm constant related to the free adsorption energy. The values of q_m and K_L were calculated from the slope and intercept of a linear fit to C_e/q_e versus C_e , respectively. Similarly the Freundlich constants K_F and $1/n$ were determined from the intercept and slope of a linear fit to $\log q_e$ versus $\log C_e$, respectively.

Langmuir and Freundlich models fitted the experimental adsorption data with the R^2 values of 0.9878 and 0.9725, respectively (Table 2). The Langmuir isotherm gave a better fit than the Freundlich isotherm.

The significant characteristics of the Langmuir isotherm can be assessed from a dimensionless constant called separation factor, R_L , which is defined by (Sadaf, & Bhatti, 2014):

$$R_L = \frac{1}{1 + K_L C_0} \quad (14)$$

The R_L was 0.3048, 0.1798, 0.1275 and 0.0988 with the four different initial CR concentrations, and all of these being in the range 0–1 indicate that the adsorption process was favorable (Lin *et al.*, 2013). In Table 2, $1/n$ was calculated from the Freundlich model and was in the range 0-1, also indicating that CR adsorption onto SMRH was favorable (Munagapati, & Kim, 2016).

3.5 Adsorption thermodynamics

In Table 3, negative values of ΔG^0 are observed, indicating that CR adsorption onto SMRH is thermodynamically spontaneous by its nature. The ΔH^0 is positive (7.305 kJ/mol), indicating that CR adsorption onto SMRH is

Table 2. Isotherm parameters for the adsorption of CR by SMRH (C_0 : 25–100 mg/L, adsorption dosage: 10 g/L, pH: 6.6–6.8, Temp: 303 K, contact time: 210 min).

Isotherm model	Parameter	Values	R^2
Langmuir	q_m (mg/g)	7.3943	0.9878
	K_L (L/mg)	0.0912	
Freundlich	R_L	0.3048	0.9725
	$1/n$	0.5033	
	K_F (mg/g)	1.0151	

Table 3. Thermodynamic parameters for the adsorption of CR by SMRH (C_0 : 100 mg/L, adsorption dosage: 10 g/L, pH: 6.6–6.8, Temp: 303–333 K, contact time: 210 min).

T (K)	ΔG^0 (kJ/mol)	ΔH^0 (kJ/mol)	ΔS^0 (J/mol.K)
303	-1.7265	7.305	29.806
313	-2.0246		
323	-2.3227		
333	-2.6207		

endothermic. Further, the positive value of ΔS^0 (29.806 J/mol.K) shows strong affinity of SMRH to CR and increasing randomness at the solid-solution interface during CR adsorption onto SMRH.

4. Conclusions

This study revealed that CTAB modified rice husk is an effective adsorbent for CR removal from aqueous solution. CR removal was strongly dependent on pH of solution, adsorbent dose, initial CR concentration, and contact time. Equilibrium studies showed that Langmuir isotherm gave a better fit to experimental data than Freundlich isotherm. The adsorption capacity of CR on SMRH was 7.39 mg/g at 303 K. Kinetic studies revealed that CR adsorption was well fit by a pseudo-second-order model. Thermodynamic studies demonstrated that CR adsorption onto SMRH was spontaneous and endothermic by its nature.

Acknowledgements

The authors gratefully acknowledge the Department of Industrial Chemistry at King Mongkut's University of Technology North Bangkok, Thailand for providing research facilities.

References

- Ansari, R., Seyghali, B., Mohammad-khah, A., & Zanjanchi, M. A. (2012). Highly efficient adsorption of anionic dyes from aqueous solutions using sawdust modified by cationic surfactant of cetyltrimethylammonium bromide. *Journal of Surfactants and Detergents*, 15(5), 557-565. doi:10.1007/s11743-012-1334-3
- Baek, M.-H., Ijagbemi, C. O., O, S.-J., & Kim, D.-S. (2010). Removal of Malachite Green from aqueous solution using degreased coffee bean. *Journal of Hazardous Materials*, 176(1–3), 820-828. doi:10.1016/j.jhazmat.2009.11.110

- Chen, H., Zhao, J., Wu, J., & Dai, G. (2011). Isotherm, thermodynamic, kinetics and adsorption mechanism studies of methyl orange by surfactant modified silkworm exuviae. *Journal of Hazardous Materials*, 192(1), 246-254. doi:10.1016/j.jhazmat.2011.05.014
- Dawood, S., & Sen, T. K. (2012). Removal of anionic dye Congo red from aqueous solution by raw pine and acid-treated pine cone powder as adsorbent: Equilibrium, thermodynamic, kinetics, mechanism and process design. *Water Research*, 46(6), 1933-1946. doi:10.1016/j.watres.2012.01.009
- Kaur, S., Rani, S., & Mahajan, R. K. (2013). Adsorption kinetics for the removal of hazardous dye Congo Red by biowaste materials as adsorbents. *Journal of Chemistry*, 2013, 12. doi:10.1155/2013/628582
- Lin, L., Zhai, S.-R., Xiao, Z.-Y., Song, Y., An, Q.-D., & Song, X.-W. (2013). Dye adsorption of mesoporous activated carbons produced from NaOH-pretreated rice husks. *Bioresource Technology*, 136(0), 437-443. doi:10.1016/j.biortech.2013.03.048
- Ludueña, L., Fasce, D., Alvarez, V. A., & Stefani, P. M. (2011). Nanocellulose from rice husk following alkaline treatment to remove silica. *BioResources*, 6(2).
- Mane, V. S., & Babu, P. V. V. (2013). Kinetic and equilibrium studies on the removal of Congo red from aqueous solution using Eucalyptus wood (*Eucalyptus globulus*) saw dust. *Journal of the Taiwan Institute of Chemical Engineers*, 44(1), 81-88. doi:10.1016/j.jtice.2012.09.013
- Munagapati, V. S., & Kim, D.-S. (2016). Adsorption of anionic azo dye Congo Red from aqueous solution by cationic modified orange peel powder. *Journal of Molecular Liquids*, 220, 540-548. doi:10.1016/j.molliq.2016.04.119
- Nandi, B. K., Goswami, A., Das, A. K., Mondal, B., & Purkait, M. K. (2008). Kinetic and equilibrium studies on the adsorption of crystal violet dye using kaolin as an adsorbent. *Separation Science and Technology*, 43(6), 1382-1403. doi:10.1080/01496390701885331
- Nassar, M. M., Daifullah, A. A., Kelany, H., & Farah, J. Y. (2015). Mass transfer study for the adsorption of hexavalent chromium using gas stirring. *International Journal of Scientific and Engineering Research*, 6(4), 826-833.
- Pathania, D., Sharma, A., & Siddiqi, Z. M. (2016). Removal of Congo red dye from aqueous system using *Phoenix dactylifera* seeds. *Journal of Molecular Liquids*, 219, 359-367. doi:10.1016/j.molliq.2016.03.020
- Roy, T. K., & Mondal, N. K. (2017). Biosorption of Congo Red from aqueous solution onto burned root of *Eichhornia crassipes* biomass. *Applied Water Science*, 7(4), 1841-1854. doi:10.1007/s13201-015-0358-z
- Sadaf, S., & Bhatti, H. N. (2014). Batch and fixed bed column studies for the removal of Indosol Yellow BG dye by peanut husk. *Journal of the Taiwan Institute of Chemical Engineers*, 45(2), 541-553. doi:10.1016/j.jtice.2013.05.004
- Safa, Y., & Bhatti, H. N. (2011). Kinetic and thermodynamic modeling for the removal of Direct Red-31 and Direct Orange-26 dyes from aqueous solutions by rice husk. *Desalination*, 272(1-3), 313-322. doi:10.1016/j.desal.2011.01.040
- Tamilselvi, S., Asaithambi, M., & Sivakumar, V. (2016). An eco-friendly non-conventional adsorbent from silk cotton fiber for the removal of methylene blue dye. *Indian Journal of Chemical Technology*, 23(6), 497-505.
- Tavlieva, M. P., Genieva, S. D., Georgieva, V. G., & Vlaev, L. T. (2013). Kinetic study of brilliant green adsorption from aqueous solution onto white rice husk ash. *Journal of Colloid and Interface Science*, 409, 112-122. doi:10.1016/j.jcis.2013.07.052
- Weber Jr., W. J., & Morris, J. C. (1963). Kinetics of Adsorption on Carbon from Solution. *Journal of the Sanitary Engineering Division*, 89(2), 31-59.
- Xi, Y., Shen, Y. F., Yang, F., Yang, G. J., Liu, C., Zhang, Z., & Zhu, D. H. (2013). Removal of azo dye from aqueous solution by a new biosorbent prepared with *Aspergillus nidulans* cultured in tobacco wastewater. *Journal of the Taiwan Institute of Chemical Engineers*, 44(5), 815-820. doi:10.1016/j.jtice.2013.01.031
- Yu, H., Wang, T., Yu, L., Dai, W., Ma, N., Hu, X., & Wang, Y. (2016). Remarkable adsorption capacity of Ni-doped magnolia-leaf-derived bioadsorbent for congo red. *Journal of the Taiwan Institute of Chemical Engineers*, 64, 279-284. doi:10.1016/j.jtice.2016.04.008
- Zenasni, M. A., Meroufel, B., Merlin, A., & George, B. (2014). Adsorption of Congo Red from aqueous solution using CTAB-Kaolin from bechar Algeria. *Journal of Surface Engineered Materials and Advanced Technology*, 4, 332-341.
- Zhang, R. D., Zhang, J. H., Zhang, X. N., Dou, C. C., & Han, R. P. (2014). Adsorption of Congo red from aqueous solutions using cationic surfactant modified wheat straw in batch mode: Kinetic and equilibrium study. *Journal of the Taiwan Institute of Chemical Engineers*, 45(5), 2578-2583. doi:10.1016/j.jtice.2014.06.009